



Adaptive structural reorientation: Developing extraordinary mechanical properties by constrained flexibility in natural materials



Zengqian Liu^{a,b,c}, Yanyan Zhang^a, Mingyang Zhang^{a,b}, Guoqi Tan^{a,b}, Yankun Zhu^a, Zhefeng Zhang^{a,b,*}, Robert O. Ritchie^{c,*}

^a Materials Fatigue and Fracture Division, Institute of Metal Research, Chinese Academy of Sciences, Shenyang 110016, China

^b School of Materials Science and Engineering, University of Science and Technology of China, Hefei 230026, China

^c Department of Materials Science and Engineering, University of California Berkeley, Berkeley, CA 94720, USA

ARTICLE INFO

Article history:

Received 4 November 2018

Received in revised form 4 January 2019

Accepted 9 January 2019

Available online 11 January 2019

Keywords:

Biomechanics

Structural reorientation

Mechanical properties

Biomaterials

Bioinspiration

ABSTRACT

Seeking strategies to enhance the overall combinations of mechanical properties is of great significance for engineering materials, but still remains a key challenge because many of these properties are often mutually exclusive. Here we reveal from the perspective of materials science and mechanics that adaptive structural reorientation during deformation, which is an operating mechanism in a wide variety of composite biological materials, functions more than being a form of passive response to allow for flexibility, but offers an effective means to simultaneously enhance rigidity, robustness, mechanical stability and damage tolerance. As such, the conflicts between different mechanical properties can be “defeated” in these composites merely by adjusting their structural orientation. The constitutive relationships are established based on the theoretical analysis to clarify the effects of structural orientation and reorientation on mechanical properties, with some of the findings validated and visualized by computational simulations. Our study is intended to give insight into the ingenious designs in natural materials that underlie their exceptional mechanical efficiency, which may provide inspiration for the development of new man-made materials with enhanced mechanical performance.

Statement of Significance

It is challenging to attain certain combinations of mechanical properties in man-made materials because many of these properties – for example, strength with toughness and stability with flexibility – are often mutually exclusive. Here we describe an effective solution utilized by natural materials, including wood, bone, fish scales and insect cuticle, to “defeat” such conflicts and elucidate the underlying mechanisms from the perspective of materials science and mechanics. We show that, by adaptation of their structural orientation on loading, composite biological materials are capable of developing enhanced rigidity, strength, mechanical stability and damage tolerance from constrained flexibility during deformation – combinations of attributes that are generally unobtainable in man-made systems. The design principles extracted from these biological materials present an unusual yet potent new approach to guide the development of new synthetic composites with enhanced combinations of mechanical properties.

© 2019 Acta Materialia Inc. Published by Elsevier Ltd. All rights reserved.

1. Introduction

The enhancement of the mechanical performance of materials is frequently restricted by a series of contradictive relationships

* Corresponding authors at: Materials Fatigue and Fracture Division, Institute of Metal Research, Chinese Academy of Sciences, Shenyang 110016, China (Z. Zhang); University of California, Berkeley, CA 94720, USA (R.O. Ritchie).

E-mail addresses: zhfzhang@imr.ac.cn (Z. Zhang), roritchie@lbl.gov (R.O. Ritchie).

between different properties, e.g., strength versus damage tolerance and the mechanical rigidity and stability versus flexibility [1]. Seeking solutions with respect to materials science to “defeat” such conflicts is highly desirable, but still remains a key challenge in man-made material-systems. However, it seems that these conflicts can be readily overcome in nature where the materials usually demonstrate outstanding combinations of mechanical properties [2,3]. In this regard, valuable inspiration may be stimulated by taking lessons from nature. Although the materials of

biological systems are “synthesized” by organisms under physiologically mild conditions using constituents with somewhat meager mechanical properties, natural materials are usually distinguished by remarkably high mechanical efficiency that is developed essentially from their ingenious designs, notably resulting from hierarchical structures with effective gradients [3–6].

A basic feature of biological materials is that most of them can be seen as composites at certain length-scales comprising at least two phases of distinct mechanical properties, particularly stiffness [6–9]. The most common motif is represented by the embedment of a stiff reinforcement, which generally has a large aspect ratio and is preferentially aligned along specific direction, within a compliant matrix, reminiscent of the synthetic fiber-reinforced composites. Prime examples of such design include the wood [9–14], bone [15–25], fish scales [26–29], and insect cuticle [30–33], the structures of which are shown in Fig. 1. Specifically, the reinforcement is present primarily in the form of, respectively, cellulose fibrils in wood cell walls, mineralized collagen fibrils in bone and fish scales, and chitin fibers in insect cuticles. The matrix phase represents the hemicellulose in the wood cell wall and non-collagenous proteins in bone, fish scales, and insect cuticles, which locate primarily at the interfaces between the constituents. The design principles behind these materials are essentially similar despite their distinctly different chemical constituents and mechanical functions.

Composite biological materials are unique and distinct compared to their man-made counterparts where mechanical properties have been systematically investigated [34–38]. For example, strong interfaces are usually a major requirement in man-made composites; nevertheless, relatively compliant and weak interfaces are preferred in biological materials for easy interfacial mobility [6,9]. The interfacial matrix between reinforcements in biological materials plays a key role in providing for the deformation of the composites. Such mechanisms, as the breakage and reformation of sacrificial bonds and the unfolding and refolding of hidden lengths, generally endow the matrix with an exceptional capability to deform, both elastically and plastically, before fracture ensues [6,9,14,39–42]. This allows the reinforcement to reorient, in particular via interfacial sliding, within the matrix in response to the loading environment. For instance, the microfibril angle (MFA),

i.e., the tilt angle of the cellulose fibrils relative to the longitudinal axis in the one of the major parts of the wood cell wall, the S2 layer, decreases by more than 10° in the *Picea abies* [L.] Karst. wood under tension, as revealed by *in situ* synchrotron x-ray diffraction analysis [14]. Another example is the scales of *Arapaima gigas* fish where the mineralized collagen fibrils can reorient towards the tensile axis by an average of $6\text{--}8^\circ$ upon loading [27,28]. Similar reorientation of mineralized collagen fibrils towards the direction of tensile stress has also been detected in human and animal bones and in annulus fibrosus tissues [20–25]. Such adaptive structural reorientation definitely provides a unique deformation mechanism in natural materials, and as such promotes flexibility. However, the precise effects of reorientation, particularly that occurring during large elastic or post-yield deformation, on the mechanical properties still remain largely unexplored in both biological and man-made composites with a lack of systematic constitutive relationships. This raises an open question whether such reorientation plays a role, in turn, in enhancing material performance and, if so, how it functions. Indeed, structural reorientation has rarely been considered as a strategy of adaptation to improve combinations of mechanical properties.

Here we reveal that structural reorientation of biological materials on loading serves more than providing a mode of passive mechanical response, but additionally offers an effective strategy to adapt their mechanical properties to better accomplish material functionality. The result is the generation of an extraordinary combination of rigidity, strength, stability and damage tolerance from constrained flexibility – combinations of attributes that are generally not available in man-made systems. Our approach is, by learning from nature, to attempt to extract the design principles which could guide the development of new bioinspired materials based on establishing systematic constitutive relationships derived with composite mechanics, and further to strive to elucidate the salient underlying mechanisms, with visualization and validation of the findings using computational simulations.

2. Theoretical model

The composite structural motif of biological materials can be described using a simple model comprising two phases that are

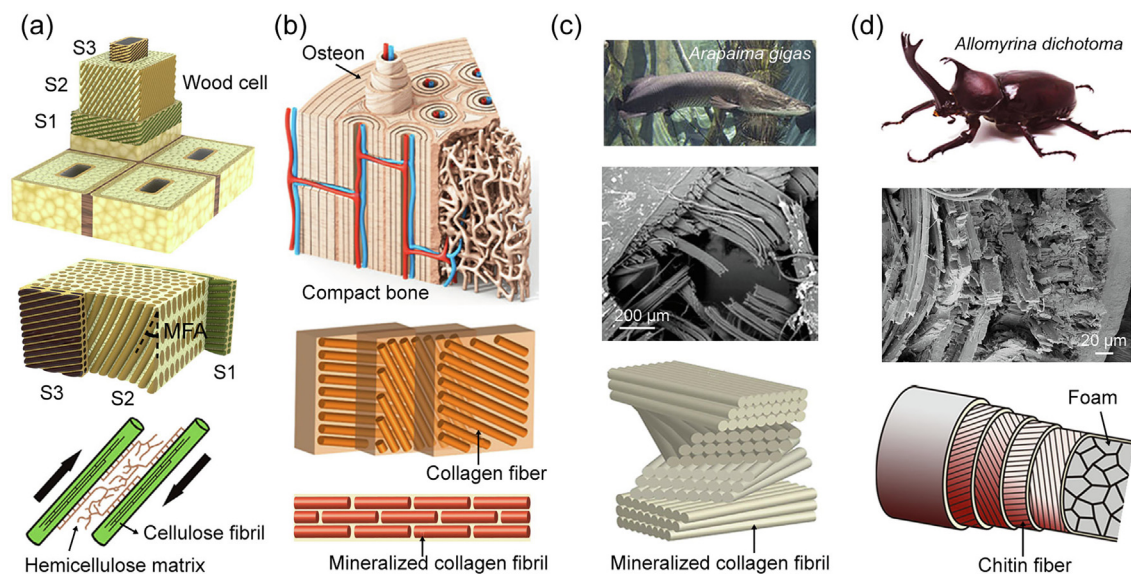


Fig. 1. Composite structural designs of representative biological materials. The reinforcement phase and interfacial matrix are present primarily in the form of the cellulose fibrils and hemicellulose in (a) wood cell wall, the mineralized collagen fibrils and non-collagenous proteins in (b) bone and (c) fish scale, and the chitin fibers and proteins in (d) insect cuticle of beetle horn. MFA in (a) denotes microfibril angle. (b) is adapted with permission from refs. [15,17]. (c) is adapted with permission from refs. [27,28].

alternately organized in two-dimensional coordinates [7,13,19,42–44], as shown in Fig. 2(a). The matrix is represented by a relatively compliant and soft phase A, which is located at the interfacial region between the stiff reinforcement B. The volume fractions of the matrix and reinforcement are denoted using V_A and V_B with $V_A + V_B = 1$; generally, the matrix accounts for the minor volume fraction in biological materials as compared to their sub-structural building blocks, giving the relation $V_A < V_B$. As any effects of structural orientation or anisotropy of the composite can be readily established by tuning the arrangement of constituents, it is reasonable to define, for simplification, the individual phases *per se* as homogeneous and isotropic. The intrinsic properties, including the elastic modulus, Poisson's ratio, density and strength, are assumed to be constant for the constituent phases. The structural orientation of the composite, which is the major variable, is depicted using the inclination angle between the longitudinal axis of constituents and the external force, θ . The Young's moduli of the matrix E_A and reinforcement E_B are defined as $E_A = 0.1$ GPa and $E_B = 2$ GPa. The volume fractions of the two phases are set to be $V_A = 0.1$ and $V_B = 0.9$. The strengths of the matrix and reinforcement are denoted, respectively, as σ_A and σ_B with $\sigma_A = 10$ MPa. The Poisson's ratio, ν , is taken to be identical between the two phases as 0.3 for simplification. It is noted that these parameters are chosen only for the purpose of giving an explicit illustration of the constitutive relationships. The varying trends and results remain constant for different values of parameters. It is difficult to correlate these parameters with specific materials as they vary significantly among different biological systems. For example, the interfacial strength σ_A is typically around 1 MPa for the interfibrillar matrix in antler bone and higher than 50 MPa for the interfaces between mineral lamellae in nacre [6,9,45]. A relatively moderate value of 10 MPa, which is of the same order as the interfaces between cellulose microfibrils in wood and the cement line in bone [6,9], is chosen here.

Although the present model is similar to man-made fiber-reinforced composites, the material attributes are markedly different in biological materials. Specifically, biological materials demonstrate microscopic mechanisms that enable easy interfacial mobility between constituents to allow for the reorientation of the reinforcement within the matrix [6,9,14,39–42]. Note here that many of the biological materials consist of multiple plies or lamellae which are stacked in a specific sequence, typically forming twisted plywood structure or even Bouligand-type structure [12,16,26–33]. This endows them with potent toughening mechanisms to enhance the fracture toughness and energy-dissipation capability. In this case, structural reorientation still occurs in each

individual lamella of the entire structure in spite of the possible friction between adjacent lamellae. On the other hand, mineralization is present in many biological materials and plays a major role in stiffening and strengthening their constituents. Taking bone and fish scales for example, the materials comprise primarily bundles of mineralized collagen fibrils which are embedded within a more compliant and weaker non-collagenous interfibrillar matrix [16–19,22,26–29]. The mineral nanoplatelets locate mainly between the heads and tails of the collagen molecules within the fibrils. In this case, the mineralized collagen fibrils can be treated as the reinforcement phase. The present model represents an elementary structural unit of a single lamella of composite where the effects of the detailed dimensions of constituents can be neglected. This enables the establishment of basic constitutive relationships to discern the effects of structural orientation and reorientation on mechanical properties. The mechanical behavior of the laminates or the entire structure of actual biological materials can be seen as an integrated response from each lamella. Indeed, structural reorientation has been experimentally detected in wood, bone and fish scales using samples comprising multiple lamellae rather than individual lamella [14,20–28].

To accommodate any deformation upon loading, the reinforcement reorients principally towards the loading direction under tension and deviates away from it under compression through the interfacial sliding (Fig. 2(b) and (c)) [14,23,24,27,28]. Such adaptability is well described, respectively, by a decrease and increase in the orientation angle θ . As such, the present model captures the primary structural characteristics of a wide variety of biological materials, especially those having fibrous, laminated, or tubular structures. In particular, the deformation mechanisms of biological materials by adaptive structural reorientation can be well described by this means. In realistic cases, there are usually multiple microscopic processes that lead to the deformation of biological materials beyond the structural reorientation. For example, mineralized collagen fibrils can be stretched both elastically and plastically along the tensile direction [25,27,28]. Additionally, strain can also be generated from the straightening of originally curved constituents during extension [27,46,47]. Here we rule out the influence of these factors by assuming the reinforcement phase to be straight and inextensible, as illustrated in Fig. 2(d). Ideally tight bonding is also defined between the reinforcement and matrix phases, signifying that their deformation is continuous at their boundaries. A quasi-static loading condition is assumed to ensure that the structure can be fully reoriented during the deformation process. Under these assumptions, the composite model is capable to reorient its structure during deformation without the

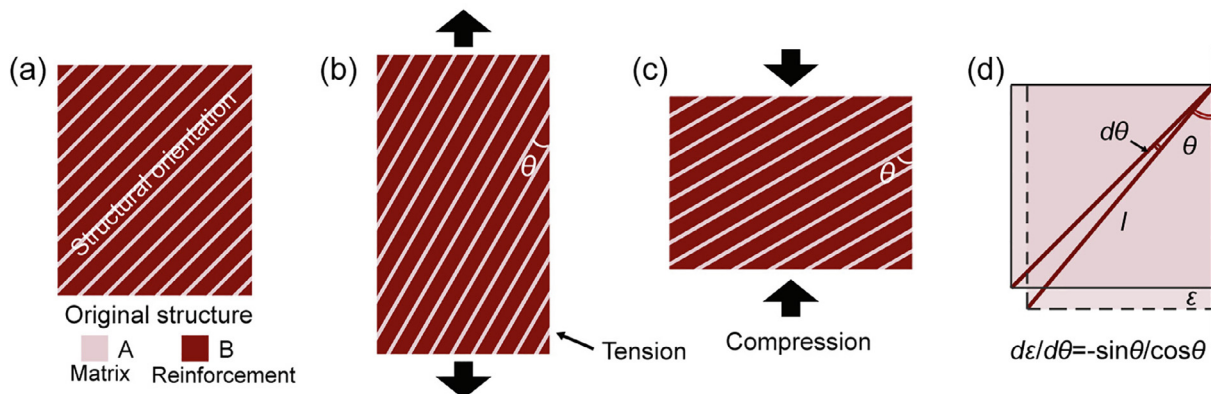


Fig. 2. Theoretical composite model for the process of adaptive structural reorientation. (a) The composite is composed of a stiff reinforcement phase B embedded within a soft matrix A. The inclination of the composite structure with respect to the loading axis θ (b) decreases under tension and (c) increases under compression. (d) Illustration of the strain ϵ resulting from the structural reorientation of a constituent with constant length l .

strain-hardening of matrix phase and the occurrence of premature fracture.

In such a scenario, the strain ε of the composite induced by structural reorientation in the process of deformation can be correlated with the structural orientation as (see Fig. 2(d)):

$$\frac{d\varepsilon}{d\theta} = -\sin\theta / \cos\theta. \quad (1)$$

This gives a solution for the strain as a function of the orientation angle θ as:

$$\varepsilon = \ln(\cos\theta / \cos\theta_0) \quad (2)$$

where θ_0 denotes the original orientation angle of the composite before deformation. The strain has a range of $\varepsilon_T \in [0, -\ln\cos\theta_0]$ for tension and $\varepsilon_C < 0$ for compression. Note here that the strain in the model composite originates merely from its adaptive structural reorientation during loading. This helps discern and clarify the effects of structural orientation and reorientation by excluding any confusion from other deformation mechanisms.

3. Tensile properties

3.1. Tensile stiffness

As a measure of the resistance of materials to elastic deformation, the stiffness of the composite is closely associated with its Young's modulus which depends on the structural orientation with respect to the loading direction [18,31,48–53]. In the case of uniaxial tension, the Young's modulus of a composite at an arbitrary orientation, E_T , has been established in our previous study considering the shear-extension coupling of the composite based on the laminate theory as [36–38,43]:

$$E_T = E_A(A\cos^4\theta + B\sin^2\theta\cos^2\theta + C\sin^4\theta)^{-1} \quad (3)$$

where k denotes the ratio between the Young's moduli of the reinforcement and matrix with $k = E_B/E_A > 1$, and $A = (V_A + k - kV_A)^{-1}$, $B = 2(1 + \nu)(kV_A + 1 - V_A)/k - 2\nu/(V_A + k - kV_A)$, and $C = (kV_A + 1 - V_A)/k$.

On loading, the structural orientation of the composite changes continuously via adaptive deformation primarily by reorienting towards the tensile direction, which leads to the variation in stiffness. The instantaneous Young's modulus of the composite during deformation can be described as a function of the tensile strain, ε_T , through integration of the above relation by incorporating Eq. (1) as:

$$E_T = E_A[(A - B + C)\cos^4\theta_0 e^{4\varepsilon_T} + (B - 2C)\cos^2\theta_0 e^{2\varepsilon_T} + C]^{-1} \quad (4)$$

where $\varepsilon_T \in [0, -\ln\cos\theta_0]$ with θ_0 being the original orientation angle. The strain-dependence of the Young's modulus, as represented by the derivative $dE_T/d\varepsilon_T$, can thus be correlated to the structural orientation as:

$$dE_T/d\varepsilon_T = 2E_T^2\cos^2\theta[(B - 2A)\cos^2\theta + (2C - B)\sin^2\theta]/E_A \quad (5)$$

A clear illustration of these relationships for the parameters $V_A = 0.1$, $E_A = 0.1\text{GPa}$, $k = 20$ and $\nu = 0.3$ is plotted in Fig. 3. As shown in Fig. 3(a), the Young's moduli of composites with differing original structural orientations can be seen to exhibit a generally increasing trend with tensile strain, specifically in a steeper fashion for a smaller original orientation angle θ_0 . This is corroborated by the general positive values of $dE_T/d\varepsilon_T$ and its negative correlation with the orientation angle (Fig. 3(b)). As such, the adaptive structural reorientation endows the composite with progressively improving stiffness and rigidity to resist more extensive elastic deformation, thus allowing for the strain-stiffening capability.

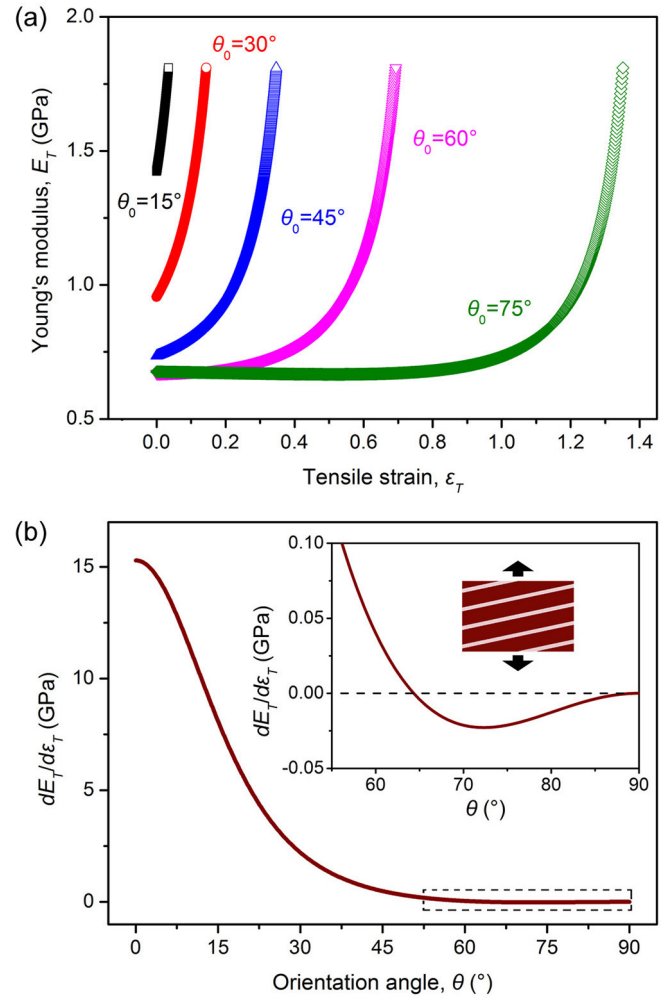


Fig. 3. Strain-stiffening behavior generated from adaptive structural reorientation. (a) Variations in the Young's moduli of composites with differing original structural orientations as a function of the tensile strain. (b) Relationship between the strain-dependence of Young's modulus and the structural orientation angle of the composite. The inset shows the magnified view of the dashed rectangular box and illustrates the tension of a composite with a high orientation angle.

Indeed, the increasing trend of Young's modulus with the decrease in misalignment between the structure and the applied load has been experimentally detected in wood, osteonal bone and beetle exoskeletons [31,48–53]. Additionally, the mechanism of reorientation of the mineralized collagen fibrils has been shown, in real time, by small-angle x-ray diffraction measurements to be active during deformation of the scales in *Arapaima gigas* fish [27,28]. Such scales, which comprise multiple lamellae, exhibit a strain-stiffening behavior under tensile loading. This agrees well with the present analysis despite the inapplicability of the quantitative relationships derived from single lamella.

Careful examination reveals that the strain dependence of the Young's modulus becomes slightly negative at high orientation angles approaching 90°, i.e., the structural orientation of composite is nearly orthogonal to the loading axis, as shown in the inset in Fig. 3(b). This implies a decreasing modulus of the composite at the initial stage of deformation as the structure reorients towards the tensile direction. Such a trend is presumed to result from the fact that the lateral Poisson's contraction of the matrix phase is tightly restricted by the reinforcement which is near-transversely aligned in the composite at the high orientation angle range. Indeed, *in situ* small-angle x-ray diffraction measurements have revealed a reverse structural reorientation in the scales of

Arapaima gigas fish of which the mineralized collagen fibrils with original orientation angles of 61–90° rotate away from the tensile direction by an average of 6.75° upon loading [27,28]. Such adaptability, despite occurring in the opposite manner to the fibrils with small orientation angles, similarly leads to an increasing Young's modulus of the composite, thereby enhancing the tensile rigidity.

3.2. Tensile strength

The strength of an orthotropic composite also demonstrates a strong dependence on its structural orientation [34–38,52–55]. In the case of uniaxial tension, the composite generally exhibits the highest strength along the longitudinal orientation, σ_l , which is generally dominated by the failure of the reinforcement [36]. For off-axis loading, the shear strength of the composite, τ_{12} , is principally governed by the sliding of the interfacial matrix. The strength of the composite subject to loading at an arbitrary direction has been correlated to the structural orientation based on the Tsai-Hill failure criterion as [43]:

$$\sigma_T = \sigma_A [\cos^4 \theta / m^2 + (m^2 - n^2) \sin^2 \theta \cos^2 \theta / (m^2 n^2) + \sin^4 \theta]^{-1/2} \quad (6)$$

with $m = \sigma_l / \sigma_A > 1$ and $n = \tau_{12} / \sigma_A$ where σ_A denotes the strength of the matrix phase. The strength displays a generally decreasing trend with increase in the inclination of the composite structure with respect to the loading axis. During the tensile deformation process, the continuous change of such inclination caused by the structural reorientation of the composite leads to a varying strength that is dependent on the tensile strain, ε_T . The instantaneous strength of composite with original orientation angle, θ_0 , can be expressed as a function of ε_T as:

$$\sigma_T = mn\sigma_A [(m^2 n^2 - m^2 + 2n^2) \cos^4 \theta_0 e^{4\varepsilon_T} + (m^2 - n^2 - 2m^2 n^2) \cos^2 \theta_0 e^{2\varepsilon_T} + m^2 n^2]^{-1/2} \quad (7)$$

The strain-dependence of the strength, $d\sigma_T/d\varepsilon_T$, can be correlated to the structural orientation following the relationship:

$$d\sigma_T/d\varepsilon_T = \sigma_T^3 \cos^2 \theta [(m^2 - 3n^2) \cos^2 \theta + (2m^2 n^2 - m^2 + n^2) \times \sin^2 \theta] / (m^2 n^2 \sigma_A^2) \quad (8)$$

The above relationships are plotted in Figure (4) using parameters of $m = 5$, $n = 0.7$ and $\sigma_A = 10\text{MPa}$. As shown in Fig. 4(a), the composites that are originally oriented at differing original orientation angles θ_0 tend to exhibit an increasing tensile strength with the increase in tensile strain during deformation. Such a characteristic enables the composite to become stronger to resist failure, thus offering improved robustness. This is reminiscent of the strain-hardening behavior of monolithic materials like metals, alloys and polymers; however, it is not associated with the property variation of constituents, but rather is generated from the adaptation of their structural orientation. Indeed, the strength has been revealed to display an increasing trend with the decreased inclination of collagen fibrils to loading in bovine cortical bones of both dry and wet states [53]. In addition, as noted above, *in situ* small-angle x-ray diffraction measurements during uniaxial tensile tests clearly show that the scales of *Arapaima gigas* fish can exhibit marked strain hardening, concomitant with distinct reorientation of the mineralized collagen fibrils [27,28]. This serves to enhance the penetration resistance and hence the protective role of the scales.

The strain-dependence of the strength, as indicated by the derivative of the strength with strain $d\sigma_T/d\varepsilon_T$, is positive at the majority of orientation range, but demonstrates a general decreasing trend with the increase in the orientation angle (Fig. 4(b)); it

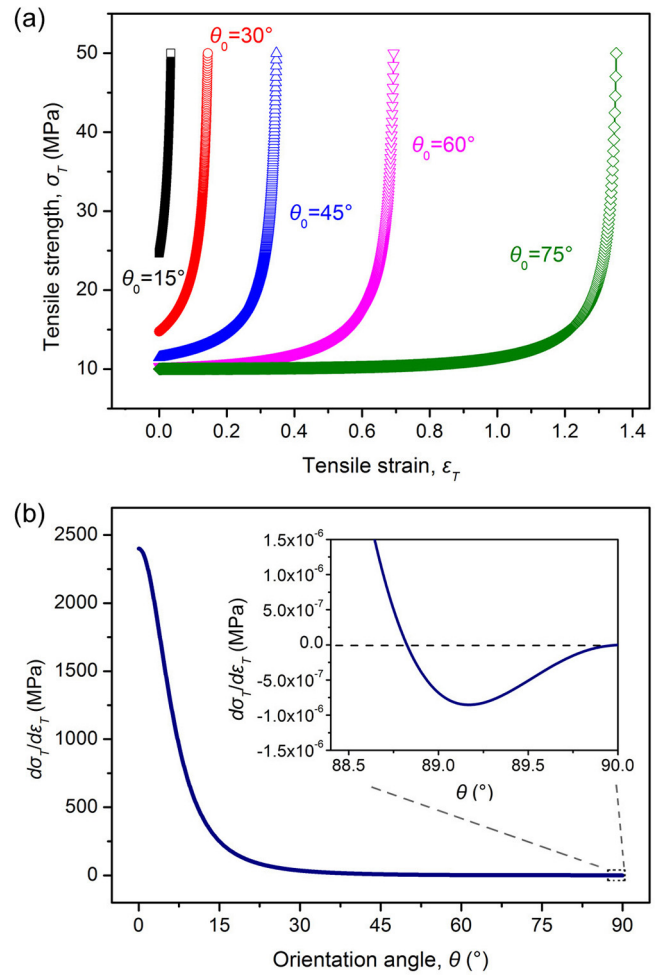


Fig. 4. Strain-hardening behavior endowed by adaptive structural reorientation. (a) Relationships between the tensile strength and the tensile strain of composites with differing original structural orientations. (b) Variation in the strain-dependence of tensile strength as a function of the orientation angle of composite. The inset is the magnified view of the dashed rectangular box.

turns slightly negative for orientations nearly orthogonal to the loading axis, similar to the effect on the Young's modulus, as shown in the inset in Fig. 4(b). This may also result from the inhibited lateral contraction of the matrix phase and is likely to lead to an apparent strain-softening behavior of the composite at the very beginning stage of deformation as its structure reorients towards the tensile direction.

3.3. Fracture resistance

Cracks in lamellar composites, especially in biological material-systems, are most commonly formed in the weak matrix or at the interfaces between the constituents [6,9,56–58]. This can be described in the present model by the cracking along the interfacial matrix phase, as illustrated in Fig. 5(a). During the deformation process in the composite, the inherent properties of the matrix phase are independent of the structural orientation, *i.e.*, it displays a constant resistance to the initiation and growth of cracks. As such, the adaptive structural reorientation of the composite has no influence on the intrinsic toughening mechanisms which are active at small length-scales ahead of the crack tip and are intimately associated with the plasticity of the matrix phase [1,59]. In this scenario, the fracture resistance of the composite is essentially dominated by the driving force for cracking generated at

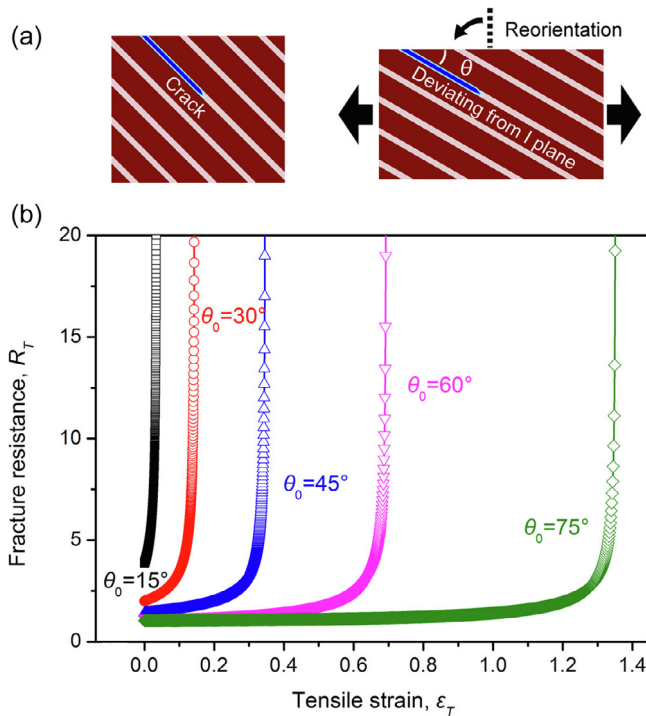


Fig. 5. Enhanced extrinsic toughening as a result of adaptive structural reorientation. (a) Schematic illustration of the deviation of the cracking path away from the mode I plane in the composite by structural reorientation. (b) Increasing fracture resistance of the composites with differing original structural orientations as a function of the tensile strain.

the crack tip from the applied load, as represented by the effective stress intensity, K_e . Any increase in K_e naturally leads to a higher propensity for fracture of the composite provided the intrinsic cracking resistance of the matrix remains the same. We can therefore evaluate the fracture resistance of the composite, R_T , using the reciprocal of the effective stress intensity according to the relation $R_T = D/K_e$ with D being a positive coefficient [43].

For the case of uniaxial tension, the effective stress intensity at the crack tip is determined primarily by the inclination of the cracking path with respect to the loading axis [60,61]. The fracture resistance of the composite can be described in terms of its structural orientation as [43]:

$$R_T = D/(K_0 \sin \theta) = D/(\varphi \sigma \sqrt{\pi c} \sin \theta) \quad (9)$$

where φ is the dimensionless geometry parameter, σ is the applied tensile stress, and c is the crack length. Here we examine the stress intensity at the tip of crack with a constant length to exclude the confusion from crack propagation. The parameter K_0 , defined by the expression $K_0 = \varphi \sigma \sqrt{\pi c}$, represents the stress intensity of an idealized crack of the same length subject to a pure mode I stress-state.

The deviation of the cracking path from the orthogonal direction in the composite, as measured by the complementary of the orientation angle θ , helps lower the effective stress intensity by shielding the crack tip from applied load. As shown in Fig. 5(a), the adaptive structural reorientation of the composite during deformation plays a role to increasingly deflect the crack from the mode I plane – the most preferred path with the maximum driving force for cracking in homogeneous materials, thus continuously enhancing the fracture resistance. The instantaneous fracture resistance of the composite in this process can be derived as a function of the apparent tensile strain as:

$$R_T = D/[K_0(1 - \cos^2 \theta_0 e^{2\epsilon_T})^{1/2}] = D/[\varphi \sigma \sqrt{\pi c}(1 - \cos^2 \theta_0 e^{2\epsilon_T})^{1/2}] \quad (10)$$

The relationships for composites with differing original structural orientations are plotted in Fig. 5(b) with the parameters D and K_0 set to unity. The fracture resistance of the composite can be seen to increase monotonically with increasing tensile strain, with a dependence that is specifically steeper at smaller θ_0 . As a major source of extrinsic toughening in many biological materials [1,17,28,61], crack deflection can constantly occur in the composite during deformation but becomes increasingly prominent as a result of the structural reorientation. This endows the material with an enhanced toughness to resist fracture which, in the case of crack propagation, is manifested by a rising crack-growth resistance curve (R-curve) behavior. The mechanism of increasing crack deflection has been observed to play an effective role in generating significant fracture toughness in the scales of striped bass *Morone saxatilis* which display marked structural reorientation of collagen fibrils during deformation [62]. Such a toughening effect may be further enhanced by considering the concomitant increase in the stiffness and strength of the composite induced by the reorientation.

4. Compressive properties

4.1. Compressive stability

In contrast to tensile loading, the load-bearing capability of composites with high-aspect-ratio constituents under compression is frequently not associated with the failure of constituents, but instead is governed by mechanical instability [44,63–65]. As a result, such composites are usually more resistant to tension than to compression loads because of the occurrence of premature buckling. The buckling acts either locally in the individual constituents, generally the reinforcement, or globally in the total composite structure, both leading to the failure of the material system [63,64], as illustrated in Fig. 6. During the process of compressive deformation, the composite adapts its structure by deviating it away from the loading axis with an increasing θ (Fig. 6(b)). Additionally, such structural reorientation leads to the increase of the load-bearing area of the component by lateral expansion – a phenomenon that is distinct from the Poisson effect (Fig. 6(c)). In the following section, we examine the separate effects of the adaptation of the composite structure with respect to its resistance to failure caused by local buckling and by global buckling. For mathematical simplification, a hollow tube model of the composite structure, which is reminiscent of the basic design of many biological material-systems such as the bird feather rachis [3,66,67], beetle horn and bone osteon [16,33,40,68], is analyzed here.

4.1.1. Local buckling resistance

The buckling of an individual constituent within the composite is caused principally by the resolved compressive stress along its axis. As illustrated in Fig. 6(b), such stress depends on the structural orientation of the composite in a manner that an increasing θ lowers the resolved axial stress for a given nominal compressive stress on the composite. The buckling strength that is intrinsic to the individual constituent in the case of axial loading, σ_c^0 , is presumed to be constant considering its fixed geometry and material properties. Accordingly, the critical stress that is sustainable by the composite, σ_c , as a measure of its resistance to local buckling, can be described in terms of the orientation angle θ as:

$$\sigma_c = \sigma_c^0 / \cos^2 \theta \quad (11)$$

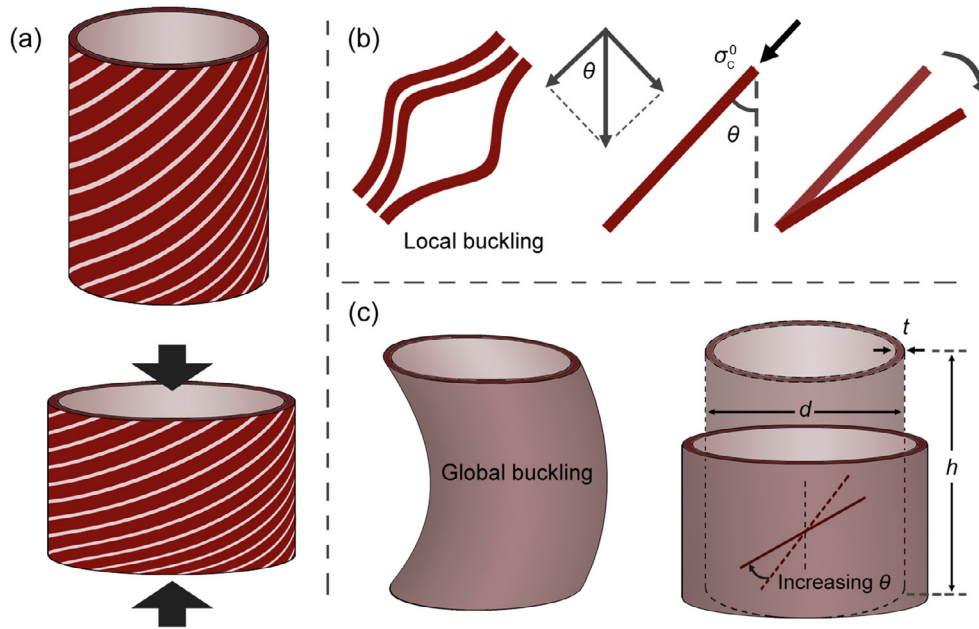


Fig. 6. Structural reorientation and mechanical instability under compression. (a) The composite structure is gradually deviated away from the loading axis during compressive deformation. This leads to (b) an increase in the local-buckling resistance and (c) a variation of the macroscopic geometry which plays a role in enhancing the global-buckling resistance.

The normalized strength of the composite, σ_c/σ_c^0 , thus is progressively increased as the orientation angle θ of its constituent is increasingly inclined with respect to the direction of compressive loading (inset in Fig. 7), indicating improved mechanical stability.

By taking the adaptive structural reorientation of the composite into account, the instantaneous local-buckling resistance during compressive deformation can be derived as a function of the compressive strain, ε_c , as:

$$\sigma_c = \sigma_c^0 (\cos^2 \theta_0 e^{2\varepsilon_c})^{-1} \quad (12)$$

with $\varepsilon_c < 0$. As shown in Fig. 7, σ_c/σ_c^0 invariably increases during compression of the composites that were originally oriented at differing θ_0 (here only the composites with small θ_0 , i.e., not exceeding 45° , are considered as buckling is more prone to occur when the

axis of constituent is close to the loading direction [36,65]). As such, the composite is capable of generating an enhanced stability to resist local buckling by reorienting its constituent to lower the axial stress. It is of note that additionally the composite's constituent is subject to another resolved compressive stress which acts along its orthogonal direction and functions to constrain its lateral deformation, thus further inhibiting the buckling. Such constraint becomes increasingly more prominent with a higher orthogonal stress which correlates positively with θ . This plays a further role in enhancing the mechanical stability of the composite against local buckling during compressive deformation. As such, the above equations are likely to give a conservative estimate of the stabilizing effect of structural reorientation in orthogonal composites.

4.1.2. Global failure resistance

Differing from the local buckling of a constituent, the resistance of the material system to failure by global buckling is largely dependent on its macroscopic geometry [65,69]. The deviation of the structure away from the compressive direction leads to the lateral expansion of the composite during deformation. With such a process, the change in the thickness of the composite (e.g., the wall thickness in the case of a tube model) can be neglected considering the fixed number of lamellae contained. The geometrical lateral expansion of the composite resulting from the structural reorientation is essentially different from the Poisson effect, as illustrated in Fig. 6(c). Indeed, the easy interfacial sliding between constituents leads to a more significant variation in the macroscopic geometry compared to the simple Poisson effect. The mechanical role of such geometrical adaptation is analyzed below by examining a tube model containing a single lamella of constituents in the wall. The tube is defined to have dimensions of height h , external diameter d , and wall thickness t (Fig. 6(c)). For simplification, the tube wall is assumed to contain one coil of constituent along the height direction with constant length l_0 , as illustrated in the inset in Fig. 8(a). As such, the height and diameter of the tube can be correlated to the structural orientation by $h = l_0 \cos \theta$ and $\pi(d - t) = l_0 \sin \theta$ where l_0 is the length of the constituent. The effective Young's modulus of the entire tube, E , is assumed to be

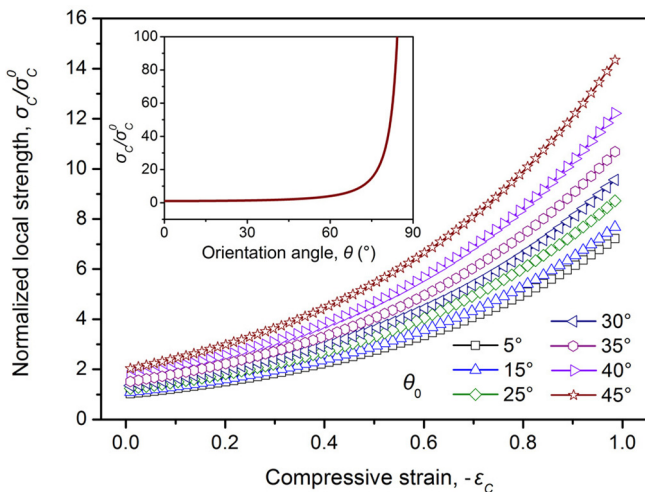


Fig. 7. Enhanced local-buckling resistance by adaptive structural reorientation. The normalized strengths of the composites with differing original structural orientations increase monotonically with the compressive strain during deformation. The inset shows the dependence of the normalized strength on the orientation angle.

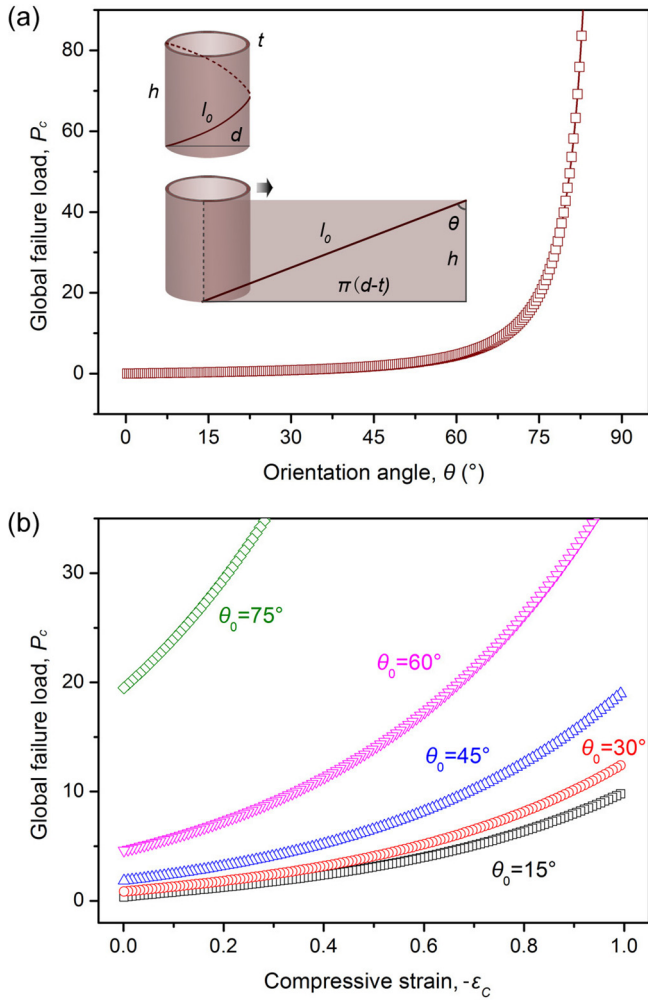


Fig. 8. Increasing global-buckling resistance during compressive deformation. (a) Dependence of the global failure load on the structural orientation angle for a tube model with height h , external diameter d , and wall thickness t . The geometry of the tube is illustrated in the inset. The tube wall contains one coil of constituent along the height direction with constant length l_0 . (b) Variations in the global failure load as a function of the compressive strain for tube models with differing original structural orientations.

constant to distinguish effects from macroscopic geometry. Then, the critical load to cause the global buckling of the system, P_C , can be described in terms of structural orientation as:

$$P_C = \pi^2 EI / h^2 = El_0 t \sin^3 \theta / (8 \cos^2 \theta) + \pi^2 Et^3 \sin \theta / (8 l_0 \cos^2 \theta), \quad (13)$$

where I is the moment of inertia of the tubular cross-section. The dependence of P_C on θ is plotted in Fig. 8(a) by setting the parameters E , l_0 , and t to unity. The increase in the inclination of the composite structure with respect to the loading direction acts to reduce the slenderness of the tube and leads to an improved mechanical stability to resist global buckling.

Lateral expansion occurs in the tube model along with a decrease of height as a result of the structural reorientation during the deformation process under compression, thereby providing a means of geometrical adaptation. The instantaneous global failure resistance P_C of the tube with original orientation angle θ_0 can be described as a function of the compressive strain ϵ_c as:

$$P_C = (1 - \cos^2 \theta_0 e^{2\epsilon_c})^{1/2} \left[(El_0^2 t + \pi^2 Et^3) / (8 l_0 \cos^2 \theta_0 e^{2\epsilon_c}) - El_0 t / 8 \right], \quad (14)$$

with $\epsilon_c < 0$. As shown in Fig. 8(b), there is a trend of increasing P_C with the increase in compressive strain in models with differing original structural orientations; specifically, the strain-dependence of P_C , as indicated by the slope of the curve, is higher for a tube with larger θ_0 . This induces a continuous improvement in the failure resistance of the tube against global buckling.

Therefore, the occurrence of buckling of the local constituents and for the entire component in the composite material-system can be inhibited by the enhanced mechanical stability developed from the respective adaptation of its microstructural orientation and macroscopic geometry. A good illustration of this is shown by wood, where the wood cell walls that are subject to compressive loading, e.g., at the lower side of tree branch, generally display a relatively large microfibril angle (MFA) which helps deviate the structure away from the loading axis [10–14]. This, in conjunction with the reorientation of cellulose fibrils during compressive deformation, is expected to help enhance the mechanical stability of wood in addition to creating internal stress by cell-wall swelling [14].

4.2. Splitting toughness

In general, brittle solids tend to fail in compression by a process of progressive micro-fracturing associated with the growth of micro-cracks [70–73]. These cracks initiate at flaws or stress concentrations within the solids, e.g., at the poles of a pore where a local tensile stress can be generated, even though the overall stress state is compressive; such cracks can then propagate in a direction which is approximately parallel to the loading direction. Macroscopic fracture occurs ultimately as a result of the linkage of the cracks and the increased volume dilatation of the solid. With respect of the present composite model, the formation and propagation of micro-cracks are assumed to be constrained within the weak matrix or by the boundaries between the matrix and the constituents – both are represented by an interfacial phase, as illustrated in Fig. 9(a). This can lead to the failure of the composite by means of splitting along the direction that conforms to its structural orientation.

In the following discussion, the splitting toughness and its dependence on the structural orientation of the composite, together with the role that adaptive structural reorientation can play, are established by analyzing the growth of an interfacial crack from a circular pore in two dimensions. The radius of the pore and the length of the crack (measured from the edge of the pore) are denoted by a and b with $L = b/a$. These dimensional parameters are assumed to be constant during the deformation process of composite to discern the effects solely from structural reorientation.

Crack propagation is mainly motivated by the axial compressive stress along its length direction, σ_1 , which creates local tensile stress at the poles of pore and at the crack tips. In addition, the crack is subject to a confining compressive stress, σ_3 , that acts in the orthogonal direction and tends to close the crack. For this configuration, the mode I stress intensity at the crack tip, K_I , can be determined by [71]:

$$K_I = \sigma_1 (\pi a L)^{1/2} \left[1.1(1 - 2.1\lambda) / (1 + L)^{3.3} - \lambda \right] \quad (15)$$

with $\lambda = \sigma_3 / \sigma_1$. The resolved stresses are correlated with the structural orientation according to $\sigma_1 = \sigma \cos^2 \theta$ and $\sigma_3 = \sigma \sin^2 \theta$, where σ is the nominal compressive stress of the composite, yielding $\lambda = \sin^2 \theta / \cos^2 \theta$. As such, the splitting resistance of the composite under compression, R_C , represented by the reciprocal of the stress intensity, can be derived similar to the treatment in Section 3.3 as a function of the orientation angle as:

$$R_C = 1/K_I = (\pi a L \sigma)^{-1/2} (1 + L)^{3.3} \left\{ 1.1 \cos^2 \theta - \left[2.31 + (1 + L)^{3.3} \right] \sin^2 \theta \right\}^{-1} \quad (16)$$

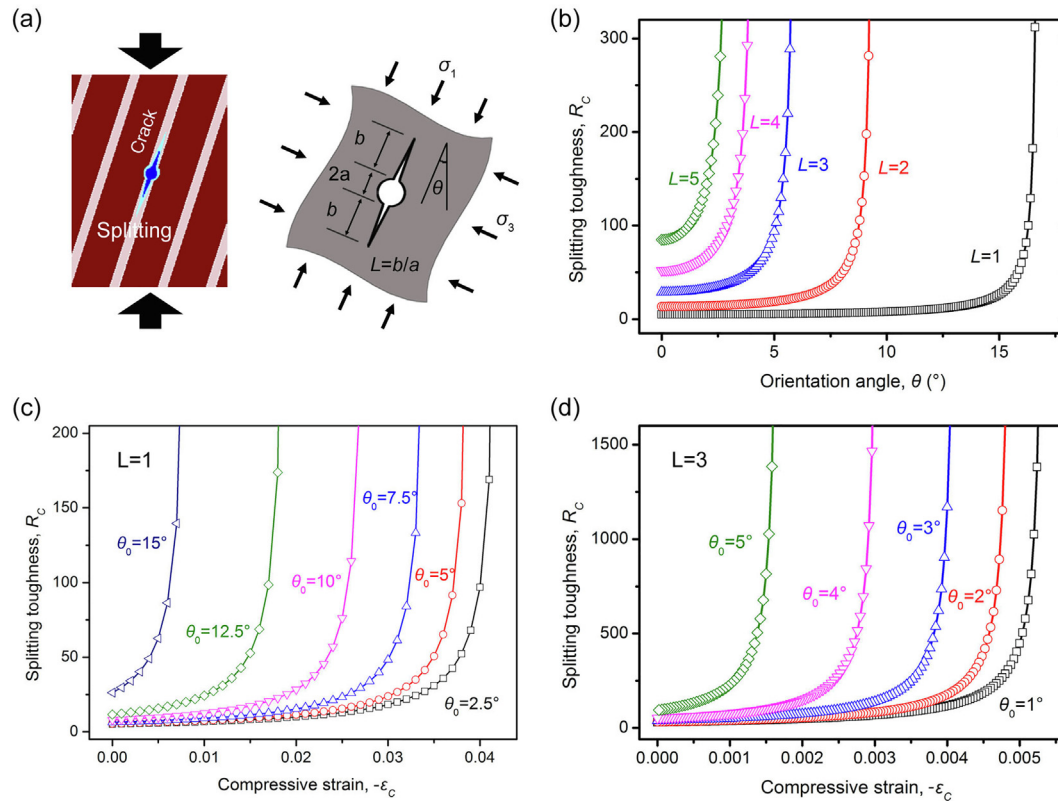


Fig. 9. Enhanced compressive splitting toughness as a result of structural reorientation. (a) Schematic illustration of the propagation of splitting cracks initiated from a pore in the interfacial matrix of the composite. (b) Dependences of the splitting toughness of composites with cracks of different dimensions on the structural orientation angle. (c, d) Variations in the splitting toughness of composites with differing original structural orientations as a function of the compressive strain in cases of relatively (c) short and (d) long cracks.

This relationship is plotted in Fig. 9(b) by setting the parameters σ and a to unity. The composite demonstrates an improved resistance against interfacial splitting, as indicated by an increasing R_C , as its structure is inclined by a larger inclination angle θ with respect to the loading direction; such a trend is especially prominent for long cracks with higher L . This effect of structural orientation on splitting toughness is corroborated by the fact that the keratin fibers that are aligned along the axial direction in the bird feather shaft of *Pavo cristatus* exhibit a high risk of splitting, especially when compared to those with large inclinations (indeed, these fibers can even play a role in resisting the splitting of feather shaft) [66,67].

The structural reorientation of the composite then can occur during the process of compressive deformation, continuously increasing the deviation of the splitting plane away from the vertical (loading) direction. This lowers the driving force for crack propagation by reducing σ_1 and simultaneously leads to a strengthened confining effect with a higher σ_3 , thus making the growth of the splitting crack increasingly more difficult. The instantaneous splitting resistance of the composite R_C can then be described in terms of the compressive strain ϵ_c as:

$$R_C = (\pi a L \sigma^2)^{-1/2} (1+L)^{3.3} \left\{ [3.41 + (1+L)^{3.3}] \cos^2 \theta_0 e^{2\epsilon_c} - 2.31 - (1+L)^{3.3} \right\}^{-1} \quad (17)$$

The variations in R_C with ϵ_c in composites with differing θ_0 for the cases of $L = 1$ and $L = 3$ are shown in Fig. 9(c) and (d). Orientations with large θ_0 are not considered here because of the preferred crack closure by the high confining stress. The composite generates an enhanced toughness by adapting its structure to resist splitting under compression. Such a toughening effect, in conjunction with

the improved fracture resistance under tension (see Section 3.3), clearly illuminates the efficiency of the composite structure in developing damage tolerance.

5. Computational simulations

Computational simulations were performed to validate and visualize part of the theoretical/analytical findings. Two-dimensional composite models with dimensions of length of 100 μm and width of 50 μm were established using the commercial finite element software ABAQUS (Dassault Systèmes, France), as shown in the inset in Fig. 10(a). One of the end boundaries of the models was fixed along the loading direction. Stiff and compliant phases were arranged in the laminated manner with the connection between them being defined with an ideally tight bonding state, *i.e.*, the deformation of the two phases was continuous at their boundaries. The lamellar thickness of the interfacial matrix and the stiff reinforcement was 1 μm and 9 μm , respectively, giving the parameters $V_A = 0.1$ and $V_B = 0.9$. Both constituent phases were considered to be linear-elastic with their Young's moduli set as $E_A = 0.1$ GPa and $E_B = 2$ GPa (giving the parameter $k = E_B/E_A = 20$) and Poisson's ratio set as $\nu = 0.3$. These are all consistent with the parameters used in the theoretical analysis. The tensile force was applied by uniformly distributing the stress on the contact boundary. Models with original orientation angles of 15°, 30°, 45°, 60°, and 75° were designed and examined for loading under uniaxial tension. In addition, side notches, with a notch width of 1 μm and a notch tip radius of 0.5 μm , were introduced into the interfacial phases at the middle sections of the composites. The projected length of the notches accounted for about half of the width of models. The notch length was set

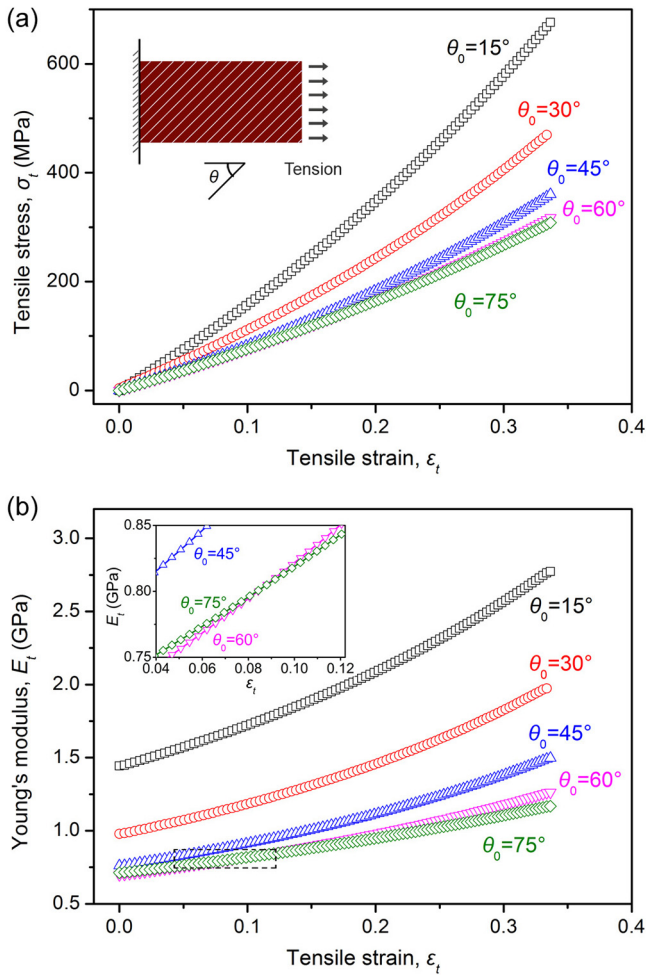


Fig. 10. Simulated mechanical properties under uniaxial tension. (a) True tensile stress-strain curves of composites with differing original structural orientations simulated using finite element analysis. The inset illustrates the composite model used in the simulation. (b) Variations in the Young's moduli of composites as a function of the tensile strain during deformation. The inset is the magnified view of the dashed rectangular box.

to be constant in the process of deformation, according to the above mechanistic analysis, to exclude the influence from cracking from the notch. Specifically, examination of notches with thickness comparable to that of the lamella of the interfacial phase, rather than sharp cracks, helps exclude the influence of factors other than the structural orientation, such as the exact position and growth direction of cracks within the interfacial phase and the severe stress concentration at the crack tips. The regions around the notch tips were finely meshed to ensure a satisfactory smoothness of the stress and strain fields.

5.1. Uniaxial tension

The true tensile stress-strain curves of the model composites obtained from the finite element simulations for differing original structural orientations are shown in Fig. 10(a). The composites display non-linear elasticity with their stress-strain curves slightly bent upwards in J-shaped fashion, implying an increasing stiffness on loading. The variation in the Young's modulus with the tensile strain for the various composites is shown in Fig. 10(b). The initial values and the varying trends of the moduli agree well with our theoretical results (Fig. 3(a)), validating the strain-stiffening behavior of the composites. Additionally, the composites with

large orientation angles exhibit an “anomalous” variation of moduli, as portrayed by the higher initial moduli of the composite with $\theta_0 = 75^\circ$ than the one with $\theta_0 = 60^\circ$ (shown in the inset). This also is consistent with the results of our analytical analysis. It is noted that the constituent material in the theoretical model is assumed to be inextensible to rule out the influence from other factors beyond the structural reorientation. As such, the strain of composite in the theoretical model originates merely from its adaptive structural reorientation during loading. However, this assumption is not applicable to the simulations where the materials can deform elastically. The strain in the modeling composite originates not only from structural reorientation, but also from the extension of constituents, and thus is invariably higher compared to the theoretical model at an equivalent stress. This leads to a decreased strain-sensitivity or strain-dependence of the modulus in the modeling than that predicted by calculation, specifically Eq. (4). As a result, an equivalent modulus can only be generated at a larger strain in the modeling, as compared to theoretical analysis, for the composites with original orientation angles of 15° and 30° where the modulus increases monotonically with strain. In contrast, for the composite with $\theta_0 = 75^\circ$, the modulus decreases initially because of the restricted lateral contraction and then increases with increasing strain in the theoretical analysis. In this case, an equivalent modulus can be generated at a smaller strain in modeling as the lateral contraction is facilitated by the deformation of the constituents. In addition, the decreased strain-dependence of the modulus in the modeling makes the two curves for $\theta_0 = 45^\circ$ and $\theta_0 = 60^\circ$ appear closer for a broader range of strain on the horizontal axis.

5.2. Fracture resistance

The influence of structural orientation on the damage tolerance of the composites can be readily accessed by comparing the stress fields corresponding to the same strain ($\varepsilon_T = 2\%$) around the tips of notches in composites with differing original orientation angles, as shown in Fig. 11(a)–(e). With the increasing inclination of the composite structure with respect to the loading axis, the stress is concentrated into smaller areas near the notch tips, as represented specifically by the narrower ranges of the high stresses. Additionally, the stress concentration sites are gradually shifted from the reinforcement phase to the weak interfacial matrix; this is also accompanied by an increase in the stress level within the interfacial phase. Accordingly, the composites with the smaller constituent orientation angles tend to possess a higher fracture resistance. Furthermore, by reorienting their structure towards the loading direction, *i.e.*, by decreasing the orientation angle, natural composites are capable of adjusting the stress fields during the deformation process. This functions to alleviate the stress concentrations at the notch tips by widening the high stress areas and shifting the stress concentration sites away from the interfacial phase. As shown in Fig. 11(e)–(h), such effects are manifested by comparing the stress fields of composites with the same original orientation angle (30°) but which are deformed at different levels of strain.

6. Conclusions

A wide variety of composite biological materials can adapt their microstructural orientation during the deformation process, generally by decreasing the inclination of their structure with respect to the loading axis under tension and increasing it under compression. Such adaptive structural reorientation is revealed here not to be simply a mode of passive response to create deformability, but also to function as a potent strategy for the natural materials

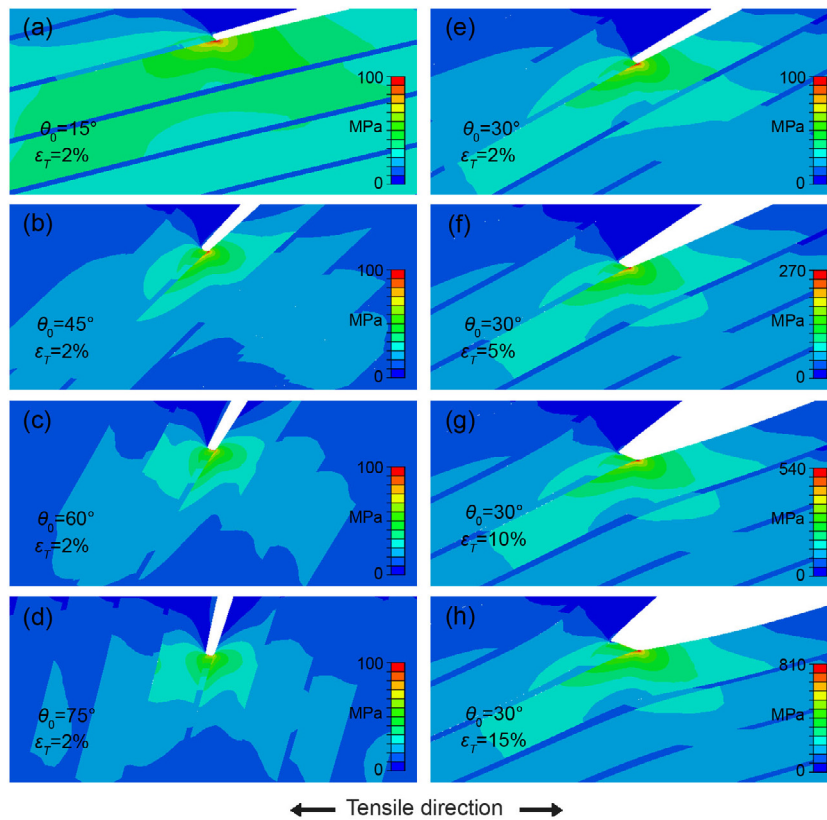


Fig. 11. Simulation of the effects of structural orientation and reorientation on damage tolerance. (a–e) Contours of the effective von Mises stress around the notch tips in composites with differing original structural orientations at the same tensile strain of 2%. (e–h) Changes in the effective von Mises stress fields around the notch tips in composites with the same original orientation angle of 30° but deformed to different strains.

to optimize their mechanical performance. These natural composites are capable of generating improved stiffness and strength during deformation under tensile loading, demonstrating their strain-stiffening and strain-hardening characteristics. At the same time, their fracture resistance can be enhanced because of a continuous deviation of the cracking path away from the mode I plane. Under compressive conditions, such structural reorientation can endow the composites with increased splitting toughness and buckling resistance of both the macroscopic component and the local microstructural constituents. This leads to the development of an enhanced combination of mechanical properties, including the rigidity, strength, stability, and damage tolerance of materials from constrained flexibility. It is of note that some of these properties are often mutually exclusive in man-made material-systems. In natural materials, conversely, such combinations of mechanical properties result essentially from their ingenious designs, including the alignment of stiff reinforcements within a compliant matrix and the presence of microscopic mechanisms that enable easy interfacial mobility (e.g., sliding) between constituents to allow for the reorientation.

In this work, constitutive relationships have been established systematically between the instantaneous mechanical properties during deformation and the corresponding strain using a theoretical/analytical analysis based on a basic composite model which was validated by computational finite element simulations. It should be noted that the current analysis is concentrated on the effects of structural orientation and reorientation by excluding the confusion from other factors. Qualitative comparison of theoretical results with experimental data in the literature does demonstrate good agreement. Nevertheless, the assumption in the theoretical model that the constituents are straight and

inextensible becomes invalid in actual biological materials. Indeed, actual biological materials are more complex, often comprise multiple lamellae with varying orientations, and deform by multiple mechanisms in addition to structural reorientation. We trust that our findings will both shed light on the strategies used by nature to develop the extraordinary mechanical properties of natural materials from the perspective of materials science and mechanics, and also suggest approaches that could be implemented in future synthetic material-systems to realize unprecedented combinations of properties.

Acknowledgements

The authors are grateful for the financial support by the National Natural Science Foundation of China under grant nos. 51871216, 11802181 and 51331007, and from the Multi-University Research Initiative under grant no. AFOSR-FA9550-15-1-0009 from the Air Force Office of Scientific Research to the University of California Riverside, specifically through a subcontract to the University of California Berkeley (for Z.L. and R.O.R.).

Competing interests statement

The authors declare no conflict of interest.

Appendix A. Supplementary data

Supplementary data to this article can be found online at <https://doi.org/10.1016/j.actbio.2019.01.010>.

References

- [1] R.O. Ritchie, The conflicts between strength and toughness, *Nat. Mater.* 10 (2011) 817–822.
- [2] U.G.K. Wegst, M.F. Ashby, The mechanical efficiency of natural materials, *Philos. Mag.* 84 (2004) 2167–2186.
- [3] M.A. Meyers, J. McKittrick, P.Y. Chen, Structural biological materials: critical mechanics-materials connections, *Science* 339 (2013) 773–779.
- [4] P. Fratzl, R. Weinkamer, Nature's hierarchical materials, *Prog. Mater. Sci.* 52 (2007) 1263–1334.
- [5] Z.Q. Liu, M.A. Meyers, Z.F. Zhang, R.O. Ritchie, Functional gradients and heterogeneities in biological materials: design principles, functions, and bioinspired applications, *Prog. Mater. Sci.* 88 (2017) 467–498.
- [6] F. Barthelat, Z. Yin, M.J. Buehler, Structure and mechanics of interfaces in biological materials, *Nat. Rev. Mater.* 1 (2016) 16007.
- [7] H. Gao, B. Ji, L.L. Jager, E. Arzt, P. Fratzl, Materials become insensitive to flaws at nanoscale: lessons from nature, *Proc. Natl. Acad. Sci. U.S.A.* 100 (2003) 5597–5600.
- [8] A.R. Studart, Biological and bioinspired composites with spatially tunable heterogeneous architectures, *Adv. Funct. Mater.* 23 (2013) 4423–4436.
- [9] J.W.C. Dunlop, R. Weinkamer, P. Fratzl, Artful interfaces within biological materials, *Mater. Today* 14 (2011) 70–78.
- [10] T. Speck, I. Burgert, Plant stems: functional design and mechanics, *Annu. Rev. Mater. Res.* 41 (2011) 169–193.
- [11] J. Farber, H.C. Lichtenegger, A. Reiterer, S. Stanzl-Tschegg, P. Fratzl, Cellulose microfibril angles in a spruce branch and mechanical implications, *J. Mater. Sci.* 36 (2001) 5087–5092.
- [12] L.J. Gibson, The hierarchical structure and mechanics of plant materials, *J. R. Soc. Interface* 9 (2012) 2749–2766.
- [13] I. Burgert, P. Fratzl, Plants control the properties and actuation of their organs through the orientation of cellulose fibrils in their cell walls, *Integr. Comp. Biol.* 49 (2009) 69–79.
- [14] J. Keckes, I. Burgert, K. Fruhmann, M. Muller, K. Kolln, M. Hamilton, M. Burghammer, S.V. Roth, S. Stanzl-Tschegg, P. Fratzl, Cell-wall recovery after irreversible deformation of wood, *Nat. Mater.* 2 (2003) 810–813.
- [15] U.G.K. Wegst, H. Bai, E. Saiz, A.P. Tomsia, R.O. Ritchie, Bioinspired structural materials, *Nat. Mater.* 14 (2015) 23–36.
- [16] S. Weiner, W. Traub, H.D. Wagner, Lamellar bone: structure-function relations, *J. Struct. Biol.* 126 (1999) 241–255.
- [17] M.E. Launey, M.J. Buehler, R.O. Ritchie, On the mechanistic origins of toughness in bone, *Annu. Rev. Mater. Res.* 40 (2010) 25–53.
- [18] H.D. Wagner, S. Weiner, On the relationship between the microstructure of bone and its mechanical stiffness, *J. Biomech.* 25 (1992) 1311–1320.
- [19] B. Ji, H. Gao, Mechanical properties of nanostructure of biological materials, *J. Mech. Phys. Solids* 52 (2004) 1963–1990.
- [20] T.M. Skerry, L. Bitensky, J. Chayen, L.E. Lanyon, Loading-related reorientation of bone proteoglycan in vivo: strain memory in bone tissue?, *J. Orthop. Res.* 6 (1988) 547–551.
- [21] G.E. Fantner, J. Adams, P. Turner, P.J. Thurner, L.W. Fisher, P.K. Hansma, Nanoscale ion mediated networks in bone: osteopontin can repeatedly dissipate large amounts of energy, *Nano Lett.* 7 (2007) 2491–2498.
- [22] S.P. Kotha, N. Guzelsu, Tensile behavior of cortical bone: dependence of organic matrix material properties on bone mineral content, *J. Biomech.* 40 (2007) 36–45.
- [23] H.A.L. Guerin, D.M. Elliott, Degeneration affects the fiber reorientation of human annulus fibrosus under tensile load, *J. Biomech.* 39 (2006) 1410–1418.
- [24] J.A. Klein, D.W.L. Hukins, Collagen fibre orientation in the annulus fibrosus of intervertebral disc during bending and torsion measured by X-ray diffraction, *Biochim. Biophys. Acta* 719 (1982) 98–101.
- [25] P.F. Yang, X.T. Nie, D.D. Zhao, Z. Wang, L. Ren, H.Y. Xu, J. Rittweger, P. Shang, Deformation regimes of collagen fibrils in cortical bone revealed by in situ morphology and elastic modulus observations under mechanical loading, *J. Mech. Behav. Biomed. Mater.* 79 (2018) 115–121.
- [26] B.J.F. Bruet, J. Song, M.C. Boyce, C. Ortiz, Materials design principles of ancient fish armour, *Nat. Mater.* 7 (2008) 748–756.
- [27] E.A. Zimmermann, B. Gludovatz, E. Schaible, N.K.N. Dave, W. Yang, M.A. Meyers, R.O. Ritchie, Mechanical adaptability of the Bouligand-type structure in natural dermal armour, *Nat. Commun.* 4 (2013) 2634.
- [28] W. Yang, V.R. Sherman, B. Gludovatz, M. Mackey, E.A. Zimmermann, E.H. Chang, E. Schaible, Z. Qin, M.J. Buehler, R.O. Ritchie, M.A. Meyers, Protective role of *Arapaima gigas* fish scales: structure and mechanical behavior, *Acta Biomater.* 10 (2014) 3599–3614.
- [29] A. Browning, C. Ortiz, M.C. Boyce, Mechanics of composite elasmoid fish scale assemblies and their bioinspired analogues, *J. Mech. Behav. Biomed. Mater.* 19 (2013) 75–86.
- [30] J.F.V. Vincent, Arthropod cuticle: a natural composite shell system, *Composites: Part A* 33 (2002) 1311–1315.
- [31] R. Yang, A. Zaheri, W. Gao, C. Hayashi, H.D. Espinosa, AFM identification of beetle exocuticle: Bouligand structure and nanofiber anisotropic elastic properties, *Adv. Funct. Mater.* 27 (2017) 1603993.
- [32] D. Raabe, C. Sachs, P. Romano, The crustacean exoskeleton as an example of a structurally and mechanically graded biological nanocomposite material, *Acta Mater.* 53 (2005) 4281–4292.
- [33] J. Zhang, G. Tan, M. Zhang, D. Jiao, Y. Zhu, S. Wang, Z. Liu, D. Liu, Z. Zhang, Multiscale designs of the chitinous nanocomposite of beetle horn towards an enhanced biomechanical functionality, *J. Mech. Behav. Biomed. Mater.* 91 (2019) 278–286.
- [34] K.H. Lo, E.S.M. Chim, Compressive strength of unidirectional composites, *J. Reinf. Plast. Comp.* 11 (1992) 838–896.
- [35] D.N. Saheb, J.P. Jog, Natural fiber polymer composites: a review, *Adv. Polym. Tech.* 18 (1999) 351–363.
- [36] R.M. Jones, *Mechanics of Composite Materials*, second ed., Taylor & Francis, Philadelphia, 1999.
- [37] V.D. Azzi, S.W. Tsai, Anisotropic strength of composites, *Exp. Mech.* 5 (1965) 283–288.
- [38] R. Hill, Theory of mechanical properties of fibre-strengthened materials: I. elastic behavior, *J. Mech. Phys. Solids* 12 (1964) 199–212.
- [39] S. Ling, D.L. Kaplan, M.J. Buehler, Nanofibrils in nature and materials engineering, *Nat. Rev. Mater.* 3 (2018) 18016.
- [40] R. Weinkamer, P. Fratzl, Mechanical adaptation of biological materials – the examples of bone and wood, *Mater. Sci. Eng. C* 31 (2011) 1164–1173.
- [41] G.E. Fantner, T. Hassenkam, J.H. Kindt, J.C. Weaver, H. Birkedal, L. Pechenik, J.A. Cutroni, G.A.G. Cidade, G.D. Stucky, D.E. Morse, P.K. Hansma, Sacrificial bonds and hidden length dissipate energy as mineralized fibrils separate during bone fracture, *Nat. Mater.* 4 (2005) 612–616.
- [42] H.S. Gupta, W. Wagermaier, G.A. Zickler, D.R.B. Aroush, S.S. Funari, P. Roschger, H.D. Wagner, P. Fratzl, Nanoscale deformation mechanisms in bone, *Nano Lett.* 5 (2005) 2108–2111.
- [43] Z.Q. Liu, Y.K. Zhu, D. Jiao, Z.Y. Weng, Z.F. Zhang, R.O. Ritchie, Enhanced protective role in materials with gradient structural orientations: lessons from nature, *Acta Biomater.* 44 (2016) 31–40.
- [44] S.E. Naleway, M.M. Porter, J. McKittrick, M.A. Meyers, Structural design elements in biological materials: application to bioinspiration, *Adv. Mater.* 27 (2015) 5455–5476.
- [45] F. Barthelat, H. Tang, P.D. Zavattieri, C.M. Li, H.D. Espinosa, On the mechanics of mother-of-pearl: a key feature in the material hierarchical structure, *J. Mech. Phys. Solids* 55 (2007) 306–337.
- [46] W. Yang, V.R. Sherman, B. Gludovatz, E. Schaible, P. Stewart, R.O. Ritchie, M.A. Meyers, On the tear resistance of skin, *Nat. Commun.* 6 (2015) 6649.
- [47] H.S. Gupta, J. Seto, W. Wagermaier, P. Zaslansky, P. Boesecke, P. Fratzl, Cooperative deformation of mineral and collagen in bone at the nanoscale, *Proc. Natl. Acad. Sci. U.S.A.* 103 (2006) 17741–17746.
- [48] I.D. Cave, L. Hutt, The anisotropic elasticity of the plant cell wall, *Wood Sci. Technol.* 2 (1968) 268–278.
- [49] A. Jager, T. Bader, K. Hofstetter, J. Eberhardsteiner, The relation between indentation modulus, microfibril angle, and elastic properties of wood cell walls, *Compos.: Part A* 42 (2011) 677–685.
- [50] C. Sachs, H. Fabritius, D. Raabe, Hardness and elastic properties of dehydrated cuticle from the lobster *Homarus americanus* obtained by nanoindentation, *J. Mater. Res.* 21 (2006) 1987–1995.
- [51] I. Burgert, Exploring the micromechanical design of plant cell wall, *Am. J. Bot.* 93 (2006) 1391–1401.
- [52] H.S. Gupta, U. Stachewicz, W. Wagermaier, P. Roschger, H.D. Wagner, P. Fratzl, Mechanical modulation at the lamellar level in osteonal bone, *J. Mater. Res.* 21 (2006) 1913–1921.
- [53] J. Seto, H.S. Gupta, P. Zaslansky, H.D. Wagner, P. Fratzl, Tough lessons from bone: extreme mechanical anisotropy at the mesoscale, *Adv. Funct. Mater.* 18 (2008) 1905–1911.
- [54] J.D. Currey, K. Brear, P. Zioupos, Dependence of mechanical properties on fibre angle in narwhal tusk, a highly oriented biological composite, *J. Biomech.* 27 (1994) 885–897.
- [55] R.B. Martin, J. Ishida, The relative effects of collagen fiber orientation, porosity, density, and mineralization on bone strength, *J. Biomech.* 22 (1989) 419–426.
- [56] Z.Y. Weng, Z.Q. Liu, R.O. Ritchie, D. Jiao, D.S. Li, H.L. Wu, L.H. Deng, Z.F. Zhang, Giant panda's tooth enamel: structure, mechanical behavior and toughening mechanisms under indentation, *J. Mech. Behav. Biomed. Mater.* 64 (2016) 125–138.
- [57] Z.Q. Liu, D. Jiao, Z.Y. Weng, Z.F. Zhang, Structure and mechanical behaviors of armored pangolin scales and the effects of hydration and orientation, *J. Mech. Behav. Biomed. Mater.* 56 (2016) 165–174.
- [58] H. Peterlik, P. Roschger, K. Klaushofer, P. Fratzl, Orientation dependent fracture toughness of lamellar bone, *Int. J. Fracture* 139 (2006) 395–405.
- [59] R.O. Ritchie, Mechanisms of fatigue-crack propagation in ductile and brittle solids, *Int. J. Fract.* 100 (1999) 55–83.
- [60] L.P. Pook, The effect of crack angle on fracture toughness, *Eng. Fract. Mech.* 3 (1971) 205–218.
- [61] R.K. Nalla, J.H. Kinney, R.O. Ritchie, Mechanistic fracture criteria for the failure of human cortical bone, *Nat. Mater.* 2 (2003) 164–168.
- [62] A.K. Dastjerdi, F. Barthelat, Teleost fish scales amongst the toughest collagenous materials, *J. Mech. Behav. Biomed. Mater.* 52 (2015) 95–107.
- [63] J.G. Davis Jr, Compressive instability and strength of uniaxial filament-reinforced epoxy tubes, *NASA-TN-D5697* (1970) 1–45.
- [64] S. Wang, J. Song, D.-H. Kim, Y. Huang, J.A. Rogers, Local versus global buckling of thin films on elastomeric substrates, *Appl. Phys. Lett.* 93 (2008) 023126.
- [65] J.M. Gere, *Mechanics of Materials*, fifth ed., China Machine Press, Beijing, 2002.
- [66] Z.Q. Liu, D. Jiao, M.A. Meyers, Z.F. Zhang, Structure and mechanical properties of naturally occurring lightweight foam-filled cylinder – the peacock's tail coverts shaft and its components, *Acta Biomater.* 17 (2015) 137–151.
- [67] T.N. Sullivan, B. Wang, H.D. Espinosa, M.A. Meyers, Extreme lightweight structures: avian feathers and bones, *Mater. Today* 20 (2017) 377–391.

- [68] Z.Q. Liu, Z.F. Zhang, R.O. Ritchie, On the materials science of nature's arms race, *Adv. Mater.* 30 (2018) 1705220.
- [69] P.M. Weaver, M.F. Ashby, Material limits for shape efficiency, *Prog. Mater. Sci.* 41 (1997) 61–128.
- [70] M.F. Ashby, S.D. Hallam, The failure of brittle solids containing small cracks under compressive stress states, *Acta Metall.* 34 (1986) 497–510.
- [71] C.G. Sammis, M.F. Ashby, The failure of brittle porous solids under compressive stress states, *Acta Metall.* 34 (1986) 511–526.
- [72] D. Jiao, Z.Q. Liu, Y.K. Zhu, Z.Y. Weng, Z.F. Zhang, Mechanical behavior of mother-of-pearl and pearl with flat and spherical laminations, *Mater. Sci. Eng. C* 68 (2016) 9–17.
- [73] S.H. Lee, C.S. Yerramalli, A.M. Waas, Compressive splitting response of glass-fiber reinforced unidirectional composites, *Compos. Sci. Technol.* 60 (2000) 2957–2966.